The Astrophysical Journal, 801:129 (11pp), 2015 March 10 doi:10.1088/0004-637X/801/2/129

PLASMA DIAGNOSTIC POTENTIAL OF $2p4f$ IN N^+—ACCURATE WAVELENGTHS AND OSCILLATOR STRENGTHS

Xiaozhi Shen[1,2], Jiguang Li[3], Per Jönsson[4], and Jianguo Wang[3]
[1] School of Physics Science and Nuclear Energy Engineering, Beihang University, Beijing 100191, China
[2] School of Mechanical and Electrical engineering, Handan College, Handan 056005, China
[3] Data Center for High Energy Density Physics, Institute of Applied Physics and Computational Mathematics, P.O. Box 8009, Beijing 100088, China; Li_Jiguang@iapcm.ac.cn
[4] Materials Science and Applied Mathematics, Malmö University, SE-20506 Malmö, Sweden
Received 2014 October 31; accepted 2014 December 31; published 2015 March 12

ABSTRACT

Radiative emission lines from nitrogen and its ions are often observed in nebula spectra, where the N^{2+} abundance can be inferred from lines of the $2p4f$ configuration. In addition, intensity ratios between lines of the $2p3p$–$2p3s$ and $2p4f$–$2p3d$ transition arrays can serve as temperature diagnostics. To aid abundance determinations and plasma diagnostics, wavelengths and oscillator strengths were calculated with high precision for electric dipole ($E1$) transitions from levels in the $2p4f$ configuration of N^+. Electron correlation and relativistic effects, including the Breit interaction, were systematically taken into account within the framework of the multiconfiguration Dirac–Hartree–Fock method. Except for the $2p4f$–$2p4d$ transitions with quite large wavelengths and the two-electron–one-photon $2p4f$–$2s2p^3$ transitions, the uncertainties of the present calculations were controlled to within 3% and 5% for wavelengths and oscillator strengths, respectively. We also compared our results with other theoretical and experimental values when available. Discrepancies were found between our calculations and previous calculations due to the neglect of relativistic effects in the latter.

Key words: atomic data – atomic processes

1. INTRODUCTION

Nitrogen is one of the most abundant elements in the universe. Radiative emission lines from nitrogen and its ions are often observed in nebula spectra, and some of the lines are suitable for abundance determinations and plasma diagnostics (Liu et al. 2000; Fang et al. 2011). In particular, there has been great interest in lines originating from levels in the $2p4f$ configuration of N^+. For example, Liu et al. determined the N^{2+}/H^+ ion abundance in NGC 6153 using the line intensities of the $2p4f$–$2p3d$ transitions (Liu et al. 2000). A similar determination was done in the Orion Nebula by Escalante and Morisset who pointed out that a major concern is the uncertainty in the line fractions involving the $2p4f$ term, where LS-coupling is not a good approximation (Escalante & Morisset 2005). Fang et al. demonstrated that the intensity ratios between the $2p3p\ ^3D$–$2p3s\ ^3P^o$ and $2p4f\ G(9/2)$–$2p3d\ ^3F^o$ transitions have a relatively strong temperature dependence, and thus can serve as temperature diagnostics (Fang et al. 2011). In addition, there exist a few lines from the $2p4f$ configuration in lightning (Wallace 1963), which play key roles in the determination of properties such as temperature and pressure (Prueitt 1963; Uman et al. 1964).

Accurate atomic parameters for the transitions from the $2p4f$ configuration are still scarce, although they are important for abundance determinations and plasma diagnostics as mentioned earlier. Mar et al. (2000) reported experimental probabilities for 20 transitions between the $2p4f$ and $2p3d$ configurations of the N^+ ion produced in a pulsed discharge lamp containing helium and nitrogen gas. However, the absolute rates were obtained by using data available in the literature as a reference (Mar et al. 2000). In addition, some experiments were carried out for measuring lifetimes of levels belonging to the $2p4f$ configuration (Denis et al. 1968; Pinnington 1970; Brink et al. 1978; Desesquelles 1971; Fink et al. 1968; McCrocklin & Head 1971). However, it is sometimes difficult to infer transition rates through lifetimes since there are always several decay channels from an individual level. Turning to theory, Kelly reported values of the single-electron integrals for the $2p4f$–$2p3d$ transitions in the Hartree–Fock–Slater approximation (Kelly 1964). Based on these data, Wiese et al. later calculated the corresponding oscillator strengths (Wiese et al. 1965). Victor and Escalante also obtained atomic parameters for the $2p4f$–$2p3d$ and $2p4f$–$2p4d$ transitions using a model potential method (Victor & Escalante 1988). Finally, as part of the Opacity Project (OP), oscillator strengths involving the $2p4f$ configuration were calculated using the R-matrix method (The Opacity Project Team 1995). However, relativistic effects were neglected in this calculation, resulting in relatively large uncertainties for the atomic parameters.

Because of the weak spin-dependent Coulomb interaction between the $2p$ and $4f$ electrons and the small spin–orbital interaction for the $4f$ electron itself, the level structure in the $2p4f$ configuration is best described as LK coupling(Cowan 1981). Also, fine-structure splittings in this configuration are extremely small. For example, the separation between the $F(5/2)_3$ and $F(5/2)_2$ levels is just $2.86\,cm^{-1}$ as shown in Figure 1. To describe this level structure, it is essential to accurately capture both relativistic and electron correlation effects. Improving on our previous work on transition probabilities from the $2p4f$ configuration (Shen et al. 2010), in which a simple correlation model was adopted, we performed large-scale calculations using the multiconfiguration Dirac–Hartree–Fock (MCDHF) method. A multireference active set approach was utilized to systematically generate the configuration space (Sturesson et al. 2007). In particular, higher-order electron correlation effects were taken into account by means of an extended set of configurations in the multireference active set (Li et al. 2012). In addition, we also considered the Breit interaction—the main relativistic correction to electron interactions (Grant 2007). The uncertainties of the present calculations were controlled to within 3% for

Table 1
The Number of CSFs (N_{CSFs}) with Different Symmetries of the Angular Momentum (J) and the Parity in Different Computational Models

Reference Configuration	AS	Model	N_{CSFs}					
			$J=0$	$J=1$	$J=2$	$J=3$	$J=4$	$J=5$
		Even						
$\{2s^22p^2; 2s^22p3p; 2s^22p4p; 2s2p^23s; 2s^22p4f;$ $2s^23d^2; 2s2p^23d; 2s2p3p3d; 2s3s3d^2; 2p^4; 2p^33p; 2p^23s3d\}$		DF	41	89	106	77	42	13
$\{2s^22p^2; 2s^22p3p; 2s^22p4p; 2s2p^23s; 2s^22p4f\}$	4	4SDV	906	2297	3020	2841	2193	1371
	5	5SDV	3064	8167	11296	11736	10251	7625
	6	6SDV	7172	19603	28028	30878	29098	23950
	7	7SDV	13808	38369	56239	64626	64425	57154
	7	7SDC	71635	200660	294281	339943	339811	303282
		Odd						
$\{2s2p^3;2s^22p3s;2s^22p3d;2s^22p4s;2s^22p4d;2s^22p5s\}$		DF	6	16	15	7	2	
	4	4SDV	1033	2727	3463	3230	2406	
	5	5SDV	3035	8255	11231	11606	9917	
	6	6SDV	7109	19682	27856	30598	28473	
	7	7SDV	13609	38147	55462	63516	62654	
	7	7SDC	68459	192172	280405	322427	319636	

Notes. AS denotes the highest principal quantum number n in the active set of orbitals. DF stands for the calculations based on the CSFs of the reference configurations. nSDV and nSDC denote the computational models.

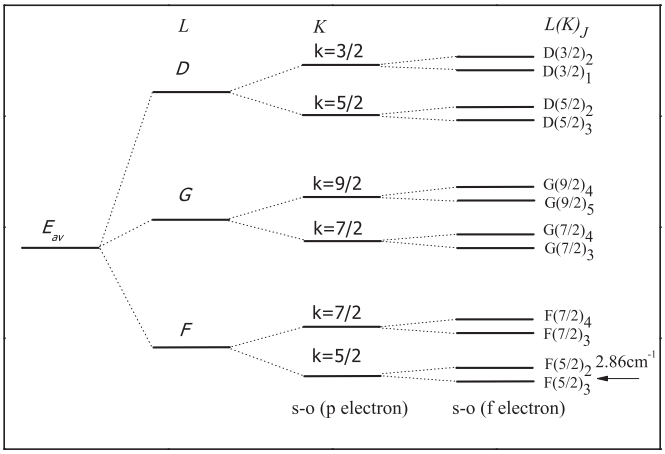

Figure 1. Energy level structure of the $2p4f$ configuration. E_{av} is the configuration's average energy. The largest interaction—the spin-independent portion of the electron–electron Coulomb interaction—gives rise to three terms F, G, and D. The spin–orbit (s–o) interaction of the $2p$ electron is the second most important interaction, and produces a separation according to the two possible values $K = L \pm s_p (s_p = 1/2)$. The s–o interaction of the $4f$ electron brings about very small splittings.

wavelengths and to about 5% for oscillator strengths of most of the lines, respectively. Based on the present work, we evaluated previous theoretical results and found some discrepancies because relativistic effects were ignored in previous calculations.

2. THEORETICAL METHOD AND COMPUTATIONAL MODEL

2.1. Theoretical Method

We employed the MCDHF method to calculate the atomic state wave functions (ASFs). The details of the method are described in the monograph by Grant (2007) and here we just give a brief account.

In the MCDHF method the ASFs are linear combinations of symmetry adapted configuration state functions (CSFs) with the same parity P and angular momentum J, and its M_J component along the z-direction:

$$\Psi(PJM_J) = \sum_{k=1}^{N_{CSFs}} c_k \Phi(\gamma_k PJM_J). \quad (1)$$

In the expression above, c_k are the expansion coefficients and γ_k denote other appropriate labeling of the CSFs, e.g., orbital occupation numbers and coupling trees. The CSFs are built from products of one-electron Dirac orbitals. In the self-consistent field procedure, both the radial parts of the Dirac orbitals and the expansion coefficients are determined to minimize the energies based on the Dirac–Coulomb Hamiltonian. Calculations can be performed for a single level, but also for a portion of a spectrum in an extended optimal level scheme, where the minimization is on a weighted sum of energies. The Breit interaction between all electron pairs is included in subsequent relativistic configuration interaction (RCI) calculations, where the radial orbitals are fixed and only the expansion coefficients are optimized (Grant et al. 1980).

For a transition between an initial i and a final f state the transition parameters such as the weighted oscillator strength gf and the transition rate A can be expressed in terms of the reduced matrix element

$$\langle \Psi_i \| O^{(L)} \| \Psi_f \rangle^2, \quad (2)$$

where $O^{(L)}$ is the multipole radiation field operator. A biorthogonal transformation technique is adopted to relax the restrictions from standard Racah algebra so that the initial and final state ASFs can be built from the different radial orbital sets (Olsen et al. 1995). All calculations were performed using the GRASP2K package (Jönsson et al. 2013) which is the latest version of GRASP (Grant et al. 1980).

2.2. Computational Model

The accuracy of MCDHF and RCI calculations is to a large extent determined by the CSF expansions. In this work, the active set approach was adopted to generate the CSF expansions. Calculations were done by parity, meaning that states of even and odd parity were optimized separately. Based on our

Table 2
Excitation Energies (in cm^{-1}) and Fine-structure Splittings (in cm^{-1}) of the $2p4f$ Configuration from Different Computational Models

Model	$F(5/2)_3$	$F(5/2)_2$	$F(7/2)_3$	$F(7/2)_4$	$G(7/2)_3$	$G(7/2)_4$	$G(9/2)_5$	$G(9/2)_4$	$D(5/2)_3$	$D(5/2)_2$	$D(3/2)_1$	$D(3/2)_2$
	($^1F_3$)	($^3F_2$)	($^3F_3$)	($^3F_4$)	($^3G_3$)	($^3G_4$)	($^3G_5$)	($^1G_4$)	($^3D_3$)	($^3D_2$)	($^3D_1$)	$^1D_2$)
Excitation energies												
DF	219061	214782	219090	219093	219337	219345	219458	219471	219473	219064	214198	219482
4SDV	205730	205730	205756	205763	205995	206004	206112	206121	206119	206122	206202	206210
5SDV	209847	209847	209873	209879	210106	210115	210220	210230	210226	210229	210307	210314
6SDV	210213	210214	210240	210245	210472	210481	210585	210596	210592	210596	210673	210680
7SDV	210326	210327	210352	210357	210586	210594	210698	210709	210710	210714	210792	210797
7SDC	210759	210760	210785	210790	211018	211027	211131	211142	211143	211147	211225	211230
7SDCB	210732	210733	210756	210761	210982	210990	211083	211094	211104	211108	211177	211182
NIST	211030	211033	211056	211060	211287	211295	211390	211402	211410	211415	211486	211490
Fine-structure splittings												
DF	−4279.06		3.62		7.70		12.71		−409.66		5284.84	
4SDV	−0.45		6.38		9.28		9.20		3.03		7.97	
5SDV	0.29		5.90		9.06		9.99		3.12		6.91	
6SDV	0.74		5.59		8.90		10.44		3.42		6.44	
7SDV	1.47		5.12		8.36		11.15		4.08		5.20	
7SDC	1.50		5.04		8.24		11.03		4.14		5.18	
7SDCB	1.50		4.77		8.33		11.10		4.18		5.17	
NIST	2.86		3.98		7.62		12.08		4.69		3.72	

Table 3
Excitation Energies (cm^{-1}) for States in the $2s2p^3$ and $2p3d$ Configurations from Different Computational Models

States	DF	4SDV	5SDV	6SDV	7SDV	7SDC	7SDCB	NIST	ξ%
$2s2p^3$									
$2s2p^3\ ^5S^o_2$	44604	44563	46842	46701	46912	46257	46227	46785	−1.19
$2s2p^3\ ^3D^o_3$	106226	99629	94148	92878	92842	92300	92253	92237	0.02
$2s2p^3\ ^3D^o_2$	106105	99623	94134	92865	92833	92290	92260	92250	0.01
$2s2p^3\ ^3D^o_1$	106027	99621	94125	92856	92827	92283	92257	92252	0.01
$2s2p^3\ ^3P^o_2$	124391	115191	111596	109999	109851	109399	109366	109218	0.14
$2s2p^3\ ^3P^o_1$	124253	115182	111583	109988	109844	109390	109360	109217	0.13
$2s2p^3\ ^3P^o_0$	124183	115178	111576	109982	109841	109386	109365	109224	0.13
$2s2p^3\ ^1D^o_2$	160740	150592	148830	146098	145719	144999	144959	144188	0.53
$2s2p^3\ ^3S^o_1$	182165	170632	159546	157086	156831	155645	155609	155127	0.31
$2s2p^3\ ^1P^o_1$	190938	180474	171356	168726	168315	167595	167562	166766	0.48
$2p3d$									
$2p3d\ ^3F^o_2$	196458	188026	186817	186042	186039	186259	186235	186512	−0.15
$2p3d\ ^3F^o_3$	196638	188112	186898	186122	186117	186339	186303	186571	−0.14
$2p3d\ ^3F^o_4$	196947	188234	187006	186231	186224	186447	186395	186652	−0.14
$2p3d\ ^1D^o_2$	197814	188697	187428	186667	186673	186848	186807	187091	−0.15
$2p3d\ ^3D^o_1$	197762	188667	187575	186903	186928	187137	187103	187438	−0.18
$2p3d\ ^3D^o_2$	198531	189038	187610	186936	186961	187170	187130	187462	−0.18
$2p3d\ ^3D^o_3$	197978	188747	187651	186979	187001	187211	187165	187492	−0.17
$2p3d\ ^3P^o_2$	199215	190175	189069	188350	188364	188576	188538	188857	−0.17
$2p3d\ ^3P^o_1$	199349	190227	189121	188402	188418	188631	188586	188909	−0.17
$2p3d\ ^3P^o_0$	199428	190255	189149	188431	188447	188661	188612	188937	−0.17
$2p3d\ ^1F^o_3$	200248	190859	189631	188878	188872	189089	189047	189335	−0.15
$2p3d\ ^1P^o_1$	203006	191901	190594	189744	189719	189928	189887	190120	−0.12

Note. ξ% is the difference between present calculations and NIST values.

experience in previous work (Shen et al. 2010) the reference configurations $2s^22p^2$, $2s^22p3p$, $2s^22p4p$, $2s2p^23s$, $2s^22p4f$ and $2s2p^3$, $2s^22p3s$, $2s^22p3d$, $2s^22p4s$, $2s^22p4d$, $2s^22p5s$ were chosen for the two parities. It is worth noting that the higher-order electron correlations can be accounted for through an extended set of reference configurations. The CSFs were formed from all configurations that could be obtained by replacing the occupied orbitals in the reference configurations with orbitals in an active set according to some rules. The rule together with the active space define the computational model. In this work we allowed single (S) and double (D) replacements from the valence orbitals as well as from the valence (V) and the $1s$ core orbitals (C); the models were denoted nSDV and nSDC, where n indicates the maximum principal quantum number of the orbitals in the active set. The orbitals in the active set were augmented layer by layer so as to be able to monitor the convergence of the physical quantities concerned. The number of CSFs is displayed in Table 1 as a function of the computational model.

Due to convergence problems in the self-consistent calculation for the even parity reference configurations, we added the following configurations $2s^23d^2$, $2s2p^23d$, $2s2p3p3d$, $2s3s3d^2$, $2p^4$, $2p^33p$, $2p^23s3d$ to stabilize the calculation. This first step is labeled DF in Table 1 only for convenience. As the active set of orbitals was enlarged, only the orbitals in the added layer were

Table 4
Line Strengths S (in a.u.) and Probabilities A (in s^{-1}) of $E1$ Transitions Involving $2p4f$ and Lower Configurations Together with the Corresponding Transition Energies ΔE in (cm^{-1})

Model	ΔE	S		A		ΔE	S		A		ΔE	S		A	
		B(len)	C(vel)	B(len)	C(vel)		B(len)	C(vel)	B(len)	C(vel)		B(len)	C(vel)	B(len)	C(vel)
							$2p4f$–$2p3d$								
		$G(7/2)_3$–$^3F^o_2$					$D(5/2)_2$–$^1P^o_1$					$F(7/2)_3$–$^3P^o_2$			
DF	22879	3.70[1]	4.14[1]	1.28[8]	1.44[8]	16058	1.39[0]	1.30[0]	2.33[6]	2.18[6]	19874	3.24[−1]	3.38[−1]	7.35[5]	7.68[5]
4SDV	17969	3.91[1]	6.80[1]	6.57[7]	1.14[8]	14222	2.25[1]	4.15[1]	2.63[7]	4.84[7]	15581	3.72[−2]	7.06[−2]	4.07[4]	7.73[4]
5SDV	23288	3.59[1]	4.03[1]	1.31[8]	1.47[8]	19636	2.22[1]	2.42[1]	6.80[7]	7.44[7]	20803	1.62[−2]	1.91[−2]	4.23[4]	4.98[4]
6SDV	24430	3.59[1]	3.72[1]	1.52[8]	1.57[8]	20852	2.17[1]	2.18[1]	7.97[7]	8.00[7]	21890	1.30[−2]	1.40[−2]	3.96[4]	4.24[4]
7SDV	24547	3.59[1]	3.59[1]	1.54[8]	1.54[8]	20995	2.17[1]	2.10[1]	8.15[7]	7.87[7]	21989	1.27[−2]	1.26[−2]	3.91[4]	3.87[4]
7SDC	24760	3.56[1]	3.50[1]	1.57[8]	1.54[8]	21219	2.18[1]	2.06[1]	8.43[7]	7.99[7]	22209	1.13[−2]	1.10[−2]	3.58[4]	3.49[4]
7SDCB	24747	3.93[1]	3.85[1]	1.72[8]	1.69[8]	21222	2.20[1]	2.08[1]	8.51[7]	8.06[7]	22218	1.17[−2]	1.13[−2]	3.70[4]	3.59[4]
NIST	24776					21295					22199				
Exp.				1.30[8]											
							$2p4f$–$2p4d$								
		$G(9/2)_5$–$^3F^o_4$					$G(9/2)_4$–$^3F^o_3$					$F(7/2)_4$–$^3D^o_3$			
5SDV	263	3.24[2]	8.26[3]	1.08[3]	2.76[4]	379	7.68[1]	1.10[3]	9.45[2]	1.35[4]					
6SDV	1274	3.26[2]	3.85[2]	1.24[5]	1.47[5]	1392	7.65[1]	8.83[1]	4.65[4]	5.36[4]	535	1.73[2]	5.58[2]	5.96[3]	1.92[4]
7SDV	1330	3.25[2]	2.66[2]	1.41[5]	1.15[5]	1449	7.65[1]	6.07[1]	5.25[4]	4.16[4]	580	1.73[2]	2.94[2]	7.64[3]	1.29[4]
7SDV	1552	3.25[2]	1.92[2]	2.24[5]	1.32[5]	1673	7.64[1]	4.50[1]	8.05[4]	4.74[4]	804	1.73[2]	1.49[2]	2.02[4]	1.74[4]
7SDCB	1555	3.25[2]	1.91[2]	2.25[5]	1.32[5]	1658	7.62[1]	4.46[1]	7.82[4]	4.57[4]	821	1.87[2]	1.59[2]	2.33[4]	1.97[4]
NIST	1566					1664					759				
							$2p4f - 2s2p^3$								
		$D(3/2)_2$–$^1P^o_1$					$D(5/2)_2$–$^1P^o_1$					$D(3/2)_2$–$^3P^o_2$			
DF	28545	2.56[0]	3.22[0]	2.41[7]	3.03[7]	28126	3.46[−1]	4.08[−1]	3.12[6]	3.68[6]	95092	1.50[−4]	1.64[−3]	5.21[4]	5.72[5]
4SDV	25736	7.08[−1]	1.24[0]	4.89[6]	8.57[6]	25649	7.73[−1]	1.36[0]	5.28[6]	9.27[6]	91019	4.11[−4]	3.25[−3]	1.26[5]	9.93[5]
5SDV	38958	1.72[−1]	2.38[−1]	4.13[6]	5.70[6]	38873	1.88[−1]	2.59[−1]	4.47[6]	6.16[6]	98718	8.68[−4]	2.13[−3]	3.38[5]	8.30[5]
6SDV	41954	1.28[−1]	1.67[−1]	3.84[6]	5.01[6]	41870	1.41[−1]	1.83[−1]	4.20[6]	5.45[6]	100681	1.13[−3]	1.94[−3]	4.67[5]	8.03[5]
7SDC	42482	1.19[−1]	1.45[−1]	3.70[6]	4.51[6]	42399	1.35[−1]	1.63[−1]	4.16[6]	5.02[6]	100946	1.28[−3]	1.82[−3]	5.32[5]	7.58[5]
7SDC	43635	1.06[−1]	1.30[−1]	3.58[6]	4.37[6]	43552	1.20[−1]	1.45[−1]	4.02[6]	4.86[6]	101831	1.20[−3]	1.73[−3]	5.12[5]	7.39[5]
7SDCB	43621	1.08[−1]	1.32[−1]	3.64[6]	4.45[6]	43547	1.21[−1]	1.46[−1]	4.04[6]	4.89[6]	101817	1.18[−3]	1.70[−3]	5.04[5]	7.28[5]
NIST	44725					44650					102273				
							$2p4f$–$2p3s$								
		$D(5/2)_3$–$^3P^o_2$					$D(3/2)_2$–$^3P^o_2$					$F(5/2)_2$–$^3P^o_1$			
DF	46955	2.25[−2]	4.26[−2]	6.74[5]	1.28[6]	46964	4.36[−2]	9.40[−2]	1.83[6]	3.95[6]	54451	1.73[−2]	1.45[−2]	1.13[6]	9.50[5]
4SDV	44499	1.63[−2]	3.83[−2]	4.15[5]	9.77[5]	44589	2.50[−2]	6.81[−2]	8.99[5]	2.45[6]	55280	1.43[−4]	4.29[−4]	9.80[3]	2.94[4]
5SDV	60610	9.66[−3]	1.96[−2]	6.22[5]	1.27[6]	60698	1.03[−3]	2.10[−3]	9.33[4]	1.90[5]	60388	1.51[−4]	2.82[−4]	1.35[4]	2.51[4]
6SDV	61908	8.90[−3]	1.62[−2]	6.11[5]	1.11[6]	61995	9.28[−4]	1.69[−3]	8.96[4]	1.63[5]	61684	1.43[−4]	2.47[−4]	1.36[4]	2.35[4]
7SDV	62037	9.57[−3]	1.52[−2]	6.61[5]	1.05[6]	62124	1.00[−3]	1.59[−3]	9.75[4]	1.54[5]	61808	1.49[−4]	2.27[−4]	1.43[4]	2.17[4]
7SDC	62251	9.31[−3]	1.49[−2]	6.50[5]	1.04[6]	62339	9.72[−4]	1.55[−3]	9.54[4]	1.52[5]	62029	1.44[−4]	2.18[−4]	1.39[4]	2.11[4]
7SDCB	62259	9.49[−3]	1.52[−2]	6.63[5]	1.06[6]	62337	9.58[−4]	1.53[−3]	9.40[4]	1.50[5]	62023	1.09[−4]	1.67[−4]	1.06[4]	1.62[4]
NIST	62334					62414					62093				
							$2p4f$–$2p4s$								
		$D(5/2)_2$–$^1P^o_1$					$D(3/2)_2$–$^3P^o_1$					$D(3/2)_1$–$^3P^o_2$			
DF	10727	5.71[−1]	4.71[−1]	2.86[5]	2.35[5]	13181	3.76[−2]	2.27[−2]	3.49[4]	2.11[4]	7451	1.48[1]	1.94[1]	4.15[6]	5.43[6]
4SDV	6899	2.20[0]	5.98[0]	2.93[5]	7.95[5]	8859	4.67[−1]	1.06[0]	1.32[5]	2.98[5]	8713	1.48[−2]	3.38[−2]	6.59[3]	1.51[4]
5SDV	12046	1.53[0]	1.57[0]	1.08[6]	1.11[6]	13543	4.29[−1]	4.37[−1]	4.32[5]	4.40[5]	13400	1.33[−2]	1.36[−2]	2.17[4]	2.21[4]
6SDV	13172	1.23[0]	1.10[0]	1.14[6]	1.02[6]	14605	3.74[−1]	3.34[−1]	4.72[5]	4.22[5]	14459	1.15[−2]	1.03[−2]	2.35[4]	2.11[4]
7SDV	13297	1.12[0]	9.63[−1]	1.07[6]	9.18[5]	14716	3.60[−1]	3.08[−1]	4.65[5]	3.98[5]	14570	1.11[−2]	9.51[−3]	2.33[4]	1.99[4]
7SDC	13552	1.11[0]	9.19[−1]	1.12[6]	9.27[5]	14935	3.63[−1]	3.01[−1]	4.89[5]	4.06[5]	14786	1.11[−2]	9.20[−3]	2.42[4]	2.01[4]
7SDCB	13554	1.11[0]	9.18[−1]	1.12[6]	9.26[5]	14914	3.46[−1]	2.87[−1]	4.65[5]	3.86[5]	14787	1.11[−2]	9.22[−3]	2.43[4]	2.01[4]
NIST	13556					14898					14775				

Notes. The number in the square bracket represents the power of 10. B(len) and C(vel) denote values in the Babushkin and Coulomb gauges, respectively. Exp. is the experimental values taken from Mar et al. (2000).

optimized. The final calculations that also allowed for substitutions from the 1s core orbital were done in RCI. For these calculations the Breit interaction was included as well.

3. RESULTS AND DISCUSSION

3.1. Excitation Energies and Fine-structure Splittings

Excitation energies of the levels in the $2p4f$ configuration, obtained with different computational models, are listed in the upper part of Table 2. The $L[K]_J$ notation is used to mark these levels. For convenience we also present the LS notation (Moore 1949). It can be found from this table that correlation effects, not only between valence electrons but also between the core and valence ones, are very important. For example, excitation energies are reduced by about 6.5% under the 4SDV model, and further adjusted by about 400 cm^{-1} when considering core–core and core–valence correlations in the 7SDC model. The influence of the Breit interaction on the excitation energies is so small

Table 5
Comparisons of the gf Term for the $2p4f$–$2p3d$ Transitions

$2p4f$–$2p3d$	gf			
	This Work	VE	OP	HFS
F–D^o	14.16	15.64	16.35	16.15
F–F^o	3.33	1.90	2.02	
G–F^o	21.07	22.27	22.98	
D–P^o	11.08	11.46	11.32	10.89
D–D^o	2.14	1.99	2.01	
D–F^o	0.10	0.06	0.05	

Note. VE, HFS, and OP are values taken from Victor & Escalante (1988), Kelly (1964), Wiese et al. (1965), and The Opacity Project Team (1995), respectively.

Table 6
The Separations (in cm^{-1}) in the F, G, and D Terms of the $2p4f$ Configuration

Array	Term Splitting (cm^{-1})		
	F	G	D
This work	26.34	101.03	74.43
OP	7.68	26.34	15.36
NIST	27.24	103.87	76.48

Note. OP are values obtained with the Opacity Project data (The Opacity Project Team 1995).

as to be negligible. Comparing with experimental values from National Institute of Standards and Technology (NIST) we see that the uncertainties are less than 0.14% for excitation energies of the $2p4f$ configuration.

As mentioned earlier, the level structure of the $2p4f$ configuration is best described in the LK-coupling scheme and the fine-structure splittings are only a few wave numbers. Therefore, the calculated fine-structure splittings are indispensable physical quantities for judging the quality of the ASFs. In the lower part of Table 2, we present the calculated splittings. One should keep in mind that these calculations were performed within the fully relativistic framework. In other words, the relativistic effects were considered from the start. As a result, the discrepancies in fine-structure splittings at the DF level is attributed to the ignored electron correlation effects. For instance, the order of the energy levels belonging to the $F(5/2)$ term is not correct until the 5SDV model has been reached. After including the Breit interaction, the calculated fine-structure splittings are in good agreement with the NIST values.

Excitation energies for levels in the $2s2p^3$ and $2p3d$ configurations are reported in Table 3 as functions of the computational models. A good agreement with the NIST values is found. The difference is overall smaller than 0.2%, except for the $2s2p^3\,^5S^o_2$, $^1D^o_2$, $^3S^o_1$, and $^1P^o_1$ states where the uncertainties approach 1%.

3.2. Transition Energies, Line Strengths, and Probabilities

In this section we investigate the influence of electron correlation effects and the Breit interaction on the electric dipole ($E1$) transitions including transition energies $\triangle E$, line strengths S, and corresponding probabilities A. In order to show these effects, the present results are shown in Table 4 for some transitions from the $2p4f$ configuration as functions of the computational models. Since the accuracy of the transition probabilities can be evaluated from the agreement between values in the Babushkin and Coulomb gauges (Ekman et al. 2014), which correspond to the length and velocity gauges in the non-relativistic limit, we also present the transition rates in these two gauges. As can be seen from Table 4, the line strengths and the transition rates of the strong lines are well converged in both gauges. Moreover, the consistency of the line strengths and transition rates in the two gauges are quite good in the 7SDCB model. In comparison with the experimental value (Mar et al. 2000), good agreement is found as well. For most of the weak lines, however, we observed that good convergence merely appear in the Babushkin (length) gauge but not in the Coulomb (velocity) gauge. Actually, it is indeed difficult to converge transition rates in the Coulomb gauge for the weak lines, since the transition operator in the Coulomb gauge is more sensitive to electron correlations than that in the Babushkin gauge. For this reason, we recommend the transition rates in the Babushkin (length) gauge to be used in astrophysical applications.

The uncertainties of the transition rates in the Babushkin (length) gauges are estimated based on the convergence trends. It is seen that the values change by about 5% from the 6SDV model to 7SDV, except for some weak lines, for example, in the $2p4f$–$2p4d$ and $2p4f$–$2s2p^3$ transition arrays. For the previous lines the small transition energies are associated with large relative uncertainties that lead to poor convergence for the transition rates that have uncertainties reaching 10%. However, these uncertainties can be reduced by rescaling the transition rates with experimental energies as we will show later. The $2p4f$–$2s2p^3$ transition is a two-electron–one-photon process and thus sensitive to electron correlation effects (Jönsson et al. 2010). In the present calculation, the uncertainty for these transitions is about 10%–15%.

3.3. Evaluations of gf for Terms of the 2p4f Configuration

Oscillator strengths for terms belonging to the $2p4f$ configuration were provided by Kelly and Wiese (Kelly 1964) and the TOPbase of OP data (The Opacity Project Team 1995). In order to evaluate the compiled data, we make comparisons with the present values. One should keep in mind that the previous calculations were non-relativistic and based on the LS-coupling scheme. Without loss of generality, we list the gf values for transitions from the $2p4f$ to the $2p3d$ configuration in Table 5. It can be seen from this table that our calculations are consistent with other results. The small discrepancies, however, are indicators of the neglected relativistic effects in previous calculations. The importance of the relativistic effects can be seen more clearly in term separations that mainly result from the spin–orbital interaction of the $2p$ electron. Using the excitation energies reported in Table 2, we obtain the term separations as the difference between the weighted average energies over the pair of levels. The values are listed in Table 6. For comparison, we also show the results obtained with NIST values. It is found that present calculations are in excellent agreement with the NIST values, but differ remarkably from the ones of the OP due to neglecting of relativistic effects and inadequate consideration of electron correlations in the latter. This means that non-relativistic calculations and the associated LS-coupling scheme are inappropriate for the case under investigation.

3.4. Atomic Parameters of the 2p4f Configuration

Wavelengths λ, weighted oscillator strengths gf, and transition probabilities A of $E1$ transitions from levels in the $2p4f$ configuration to all lower-lying levels in N^+ are reported in

Table 7
Wavelengths λ, Weighted Oscillator Strengths gf, and Transition Probabilities A of $E1$ Transitions from the $2p4f$ Configuration

Upper	Lower	λ (nm)			gf	A (s^{-1})		
		Calc.	Obs.	ξ%		Calc.	Exp	σ[a]
				$2p4f$–$2s2p^3$				
$2p4f\,D(3/2)_1$	$2s2p^3\ ^3P^o_0$	98.220	97.787	0.44	9.23[−4]	2.13[6]		
$2p4f\,D(3/2)_1$	$2s2p^3\ ^3P^o_1$	98.216	97.780	0.45	6.93[−4]	1.60[6]		
$2p4f\,F(5/2)_2$	$2s2p^3\ ^3D^o_1$	84.405	84.188	0.26	2.63[−3]	4.93[6]		
$2p4f\,D(5/2)_2$	$2s2p^3\ ^3P^o_1$	98.282	97.849	0.44	9.23[−4]	1.27[6]		
$2p4f\,D(3/2)_2$	$2s2p^3\ ^3P^o_1$	98.211	97.777	0.44	1.10[−3]	1.52[6]		
$2p4f\,F(5/2)_2$	$2s2p^3\ ^1P^o_1$	231.634	225.901	2.54	1.02[−3]	2.53[5]		
$2p4f\,D(5/2)_2$	$2s2p^3\ ^1P^o_1$	229.638	223.967	2.53	1.60[−2]	4.04[6]		
$2p4f\,D(3/2)_2$	$2s2p^3\ ^1P^o_1$	229.249	223.590	2.53	1.44[−2]	3.64[6]		
$2p4f\,D(5/2)_2$	$2s2p^3\ ^1D^o_2$	151.173	148.749	1.63	1.79[−3]	1.05[6]		
$2p4f\,D(3/2)_2$	$2s2p^3\ ^1D^o_2$	151.004	148.583	1.63	1.61[−3]	9.42[5]		
$2p4f\,F(5/2)_3$	$2s2p^3\ ^3D^o_2$	84.409	84.189	0.26	1.89[−3]	2.52[6]		
$2p4f\,F(7/2)_3$	$2s2p^3\ ^3D^o_2$	84.391	84.171	0.26	1.85[−3]	2.48[6]		
$2p4f\,D(5/2)_3$	$2s2p^3\ ^3P^o_2$	98.291	97.854	0.45	3.62[−3]	3.57[6]		
$2p4f\,F(5/2)_3$	$2s2p^3\ ^1D^o_2$	152.039	149.606	1.63	1.66[−2]	6.86[6]		
$2p4f\,F(7/2)_3$	$2s2p^3\ ^1D^o_2$	151.982	149.548	1.63	1.40[−2]	5.78[6]		
$2p4f\,G(7/2)_3$	$2s2p^3\ ^1D^o_2$	151.463	149.033	1.63	2.20[−3]	9.12[5]		
$2p4f\,D(5/2)_3$	$2s2p^3\ ^1D^o_2$	151.182	148.760	1.63	7.43[−4]	3.10[5]		
$2p4f\,D(5/2)_3$	$2s2p^3\ ^3D^o_3$	84.139	83.911	0.27	7.76[−4]	1.04[6]		
$2p4f\,F(7/2)_4$	$2s2p^3\ ^3D^o_3$	84.382	84.159	0.27	4.88[−3]	5.08[6]		
$2p4f\,G(7/2)_4$	$2s2p^3\ ^3D^o_3$	84.219	83.993	0.27	6.26[−4]	6.54[5]		
				$2p4f$–$2p3s$				
$2p4f\,D(3/2)_2$	$2p3s\ ^3P^o_1$	160.071	159.872	0.12	5.04[−4]	2.62[5]		
$2p4f\,D(5/2)_3$	$2p3s\ ^3P^o_2$	160.618	160.426	0.12	1.79[−3]	6.63[5]		
				$2p4f$–$2p3d$				
$2p4f\,D(3/2)_1$	$2p3d\ ^3P^o_0$	443.157	443.472	−0.07	9.30[−1]	1.05[8]		
$2p4f\,D(3/2)_1$	$2p3d\ ^3D^o_1$	415.378	415.817	−0.11	1.96[−1]	2.53[7]		
$2p4f\,D(3/2)_1$	$2p3d\ ^3P^o_1$	442.645	442.921	−0.06	7.23[−1]	8.21[7]		
$2p4f\,F(5/2)_2$	$2p3d\ ^3D^o_1$	423.182	423.812	−0.15	2.44[0]	1.81[8]		
$2p4f\,D(5/2)_2$	$2p3d\ ^3D^o_1$	416.568	417.056	−0.12	1.18[−2]	9.07[5]		
$2p4f\,D(3/2)_2$	$2p3d\ ^3D^o_1$	415.289	415.753	−0.11	5.03[−2]	3.89[6]		
$2p4f\,F(5/2)_2$	$2p3d\ ^3P^o_1$	451.517	452.003	−0.11	2.83[−2]	1.85[6]		
$2p4f\,D(5/2)_2$	$2p3d\ ^3P^o_1$	443.996	444.326	−0.07	1.01[0]	6.83[7]	6.95[7]	16%
			444.20[a]					
$2p4f\,D(3/2)_2$	$2p3d\ ^3P^o_1$	442.544	442.848	−0.07	1.03[0]	7.01[7]	5.68[7]	50%
			442.72[a]					
$2p4f\,F(5/2)_2$	$2p3d\ ^1P^o_1$	479.694	478.179	0.32	6.55[−2]	3.80[6]		
			478.043[b]					
$2p4f\,D(5/2)_2$	$2p3d\ ^1P^o_1$	471.214	469.596	0.34	1.42[0]	8.51[7]	6.07[7]	12%
			469.46[a]					
$2p4f\,D(3/2)_2$	$2p3d\ ^1P^o_1$	469.577	467.944	0.35	1.45[0]	8.77[7]		
$2p4f\,D(3/2)_1$	$2p3d\ ^3F^o_2$	400.920	400.400	0.13	8.64[−3]	1.20[6]		
$2p4f\,D(3/2)_1$	$2p3d\ ^3D^o_2$	415.846	416.233	−0.09	7.15[−2]	9.19[6]		
$2p4f\,D(3/2)_1$	$2p3d\ ^3P^o_2$	441.720	441.907	−0.04	5.19[−2]	5.92[6]		
$2p4f\,F(5/2)_2$	$2p3d\ ^3F^o_2$	408.185	407.808	0.09	2.64[−1]	2.12[7]	8.00[6]	42%
			407.69[a]					
$2p4f\,F(5/2)_2$	$2p3d\ ^1D^o_2$	417.949	417.684	0.06	1.39[−2]	1.06[6]		
$2p4f\,D(5/2)_2$	$2p3d\ ^1D^o_2$	411.497	411.120	0.09	2.24[−1]	1.76[7]		
$2p4f\,D(3/2)_2$	$2p3d\ ^1D^o_2$	410.249	409.854	0.10	2.30[−1]	1.82[7]		
$2p4f\,F(5/2)_2$	$2p3d\ ^3D^o_2$	423.667	424.243	−0.14	3.42[−1]	2.54[7]		
$2p4f\,D(5/2)_2$	$2p3d\ ^3D^o_2$	417.038	417.474	−0.10	3.09[−1]	2.37[7]	1.20[7]	30%
			417.36[a]					
$2p4f\,D(3/2)_2$	$2p3d\ ^3D^o_2$	415.756	416.168	−0.10	1.27[−1]	9.77[6]		
$2p4f\,F(5/2)_2$	$2p3d\ ^3P^o_2$	450.555	450.947	−0.09	8.59[−3]	5.65[5]		
$2p4f\,D(5/2)_2$	$2p3d\ ^3P^o_2$	443.065	443.306	−0.05	3.18[−1]	2.16[7]		
$2p4f\,D(3/2)_2$	$2p3d\ ^3P^o_2$	441.619	441.834	−0.05	4.16[−1]	2.85[7]	2.33[7]	14%
			441.71[a]					
$2p4f\,F(7/2)_3$	$2p3d\ ^3F^o_2$	407.805	407.420	0.09	9.66[−1]	5.54[7]	4.99[7]	19%
			407.30[a]					
$2p4f\,G(7/2)_3$	$2p3d\ ^3F^o_2$	404.085	403.622	0.11	2.95[0]	1.72[8]	1.30[8]	7%
			403.51[a]					
$2p4f\,F(5/2)_3$	$2p3d\ ^1D^o_2$	417.975	417.734	0.06	2.22[0]	1.21[8]	1.13[8]	19%
			417.62[a]					
$2p4f\,F(7/2)_3$	$2p3d\ ^1D^o_2$	417.552	417.277	0.07	1.14[0]	6.24[7]	4.48[7]	11%

Table 7
(Continued)

Upper	Lower	λ (nm)			gf	A (s^{-1})		
		Calc.	Obs.	ξ%		Calc.	Exp	σ[a]
			417.16[a]					
$2p4fG(7/2)_3$	$2p3d\ ^1D^o_2$	413.652	413.294	0.09	4.08[−1]	2.27[7]	2.04[7]	13%
			413.18[a]					
$2p4fD(5/2)_3$	$2p3d\ ^1D^o_2$	411.568	411.199	0.09	5.34[−2]	3.00[6]		
$2p4fF(5/2)_3$	$2p3d\ ^3D^o_2$	423.694	424.295	−0.14	1.53[0]	8.12[7]		
$2p4fF(7/2)_3$	$2p3d\ ^3D^o_2$	423.258	423.824	−0.13	1.79[0]	9.55[7]		
$2p4fG(7/2)_3$	$2p3d\ ^3D^o_2$	419.252	419.715	−0.11	3.14[−1]	1.70[7]		
$2p4fD(5/2)_3$	$2p3d\ ^3D^o_2$	417.111	417.556	−0.11	2.08[−3]	1.14[5]		
$2p4fF(5/2)_3$	$2p3d\ ^3P^o_2$	450.585	451.005	−0.09	1.22[−1]	5.74[6]		
$2p4fF(7/2)_3$	$2p3d\ ^3P^o_2$	450.093	450.473	−0.08	7.86[−4]	3.70[4]		
$2p4fD(5/2)_3$	$2p3d\ ^3P^o_2$	443.147	443.398	−0.06	3.73[0]	1.81[8]		
$2p4fF(5/2)_2$	$2p3d\ ^3F^o_3$	409.326	408.798	0.13	2.63[−2]	2.10[6]		
$2p4fD(5/2)_2$	$2p3d\ ^3F^o_3$	403.135	402.509	0.16	1.30[−2]	1.07[6]		
$2p4fD(3/2)_2$	$2p3d\ ^3F^o_3$	401.937	401.295	0.16	6.78[−3]	5.60[5]		
$2p4fF(5/2)_2$	$2p3d\ ^3D^o_3$	424.300	424.790	−0.12	6.15[−3]	4.56[5]		
$2p4fD(5/2)_2$	$2p3d\ ^3D^o_3$	417.652	418.003	−0.08	4.86[−2]	3.72[6]		
$2p4fD(3/2)_2$	$2p3d\ ^3D^o_3$	416.366	416.694	−0.08	4.19[−2]	3.23[6]		
$2p4fF(5/2)_2$	$2p3d\ ^1F^o_3$	461.115	460.877	0.05	5.19[−4]	3.25[4]		
$2p4fD(5/2)_2$	$2p3d\ ^1F^o_3$	453.274	452.899	0.08	9.48[−3]	6.16[5]		
$2p4fD(3/2)_2$	$2p3d\ ^1F^o_3$	451.760	451.363	0.09	9.85[−3]	6.44[5]		
$2p4fF(5/2)_3$	$2p3d\ ^3F^o_3$	409.351	408.846	0.12	1.93[−1]	1.10[7]		
$2p4fF(7/2)_3$	$2p3d\ ^3F^o_3$	408.944	408.409	0.13	3.52[−2]	2.01[6]		
$2p4fG(7/2)_3$	$2p3d\ ^3F^o_3$	405.203	404.592	0.15	4.50[−1]	2.61[7]	2.14[7]	39%
			404.48[a]					
$2p4fF(5/2)_3$	$2p3d\ ^3D^o_3$	424.327	424.842	−0.12	7.84[−2]	4.15[6]		
$2p4fF(7/2)_3$	$2p3d\ ^3D^o_3$	423.891	424.370	−0.11	2.13[−1]	1.13[7]		
$2p4fG(7/2)_3$	$2p3d\ ^3D^o_3$	419.872	420.251	−0.09	3.91[−2]	2.11[6]		
$2p4fD(5/2)_3$	$2p3d\ ^3D^o_3$	417.725	418.085	−0.09	7.75[−1]	4.23[7]	4.70[7]	23%
			417.97[a]					
$2p4fF(5/2)_3$	$2p3d\ ^1F^o_3$	461.147	460.938	0.05	2.64[−1]	1.18[7]		
$2p4fF(7/2)_3$	$2p3d\ ^1F^o_3$	460.631	460.382	0.05	2.16[−1]	9.69[6]		
$2p4fG(7/2)_3$	$2p3d\ ^1F^o_3$	455.890	455.538	0.08	4.04[−2]	1.85[6]		
$2p4fD(5/2)_3$	$2p3d\ ^1F^o_3$	453.360	452.995	0.08	1.73[−2]	8.03[5]		
$2p4fF(7/2)_4$	$2p3d\ ^3F^o_3$	408.865	408.342	0.13	8.18[−1]	3.63[7]	3.35[7]	16%
			408.23[a]					
$2p4fG(7/2)_4$	$2p3d\ ^3F^o_3$	405.066	404.467	0.15	2.65[0]	1.20[8]	1.25[8]	25%
			404.35[a]					
$2p4fG(9/2)_4$	$2p3d\ ^3F^o_3$	403.375	402.722	0.16	1.68[0]	7.65[7]	6.72[7]	15%
			402.61[a]					
$2p4fF(7/2)_4$	$2p3d\ ^3D^o_3$	423.805	424.298	−0.12	4.39[0]	1.81[8]		
			424.1[c]					
$2p4fG(7/2)_4$	$2p3d\ ^3D^o_3$	419.725	420.116	−0.09	6.90[−1]	2.90[7]		
$2p4fG(9/2)_4$	$2p3d\ ^3D^o_3$	417.910	418.233	−0.08	6.76[−3]	2.87[5]		
$2p4fF(7/2)_4$	$2p3d\ ^1F^o_3$	460.530	460.297	0.05	2.27[−1]	7.95[6]		
$2p4fG(7/2)_4$	$2p3d\ ^1F^o_3$	455.717	455.380	0.07	1.91[0]	6.80[7]	6.11[7]	9%
			455.25[a]					
$2p4fG(9/2)_4$	$2p3d\ ^1F^o_3$	453.577	453.168	0.09	4.20[0]	1.51[8]	1.45[8]	20%
			453.04[a]					
$2p4fF(5/2)_3$	$2p3d\ ^3F^o_4$	410.903	410.213	0.17	8.97[−3]	5.06[5]		
$2p4fF(7/2)_3$	$2p3d\ ^3F^o_4$	410.493	409.773	0.18	1.05[−2]	5.91[5]		
$2p4fG(7/2)_3$	$2p3d\ ^3F^o_4$	406.724	405.931	0.20	1.26[−2]	7.23[5]		
$2p4fD(5/2)_3$	$2p3d\ ^3F^o_4$	404.708	403.910	0.20	3.46[−2]	2.01[6]		
$2p4fF(7/2)_4$	$2p3d\ ^3F^o_4$	410.413	409.706	0.17	3.01[−1]	1.33[7]		
$2p4fG(7/2)_4$	$2p3d\ ^3F^o_4$	406.586	405.805	0.19	4.78[−1]	2.14[7]	1.99[7]	20%
			405.69[a]					
$2p4fG(9/2)_4$	$2p3d\ ^3F^o_4$	404.882	404.048	0.21	1.08[−1]	4.90[6]		
$2p4fG(9/2)_5$	$2p3d\ ^3F^o_4$	405.064	404.245	0.20	6.59[0]	2.44[8]	2.08[8]	10%
			404.13[a]					
				$2p4f$–$2p4s$				
$2p4fD(3/2)_1$	$2p4s\ ^3P^o_0$	668.378	669.060	−0.10	1.03[−2]	5.11[5]		
$2p4fD(3/2)_1$	$2p4s\ ^3P^o_1$	670.747	671.388	−0.10	7.61[−3]	3.76[5]		
$2p4fD(5/2)_2$	$2p4s\ ^3P^o_1$	673.855	674.623	−0.11	7.25[−3]	2.13[5]		
$2p4fD(3/2)_2$	$2p4s\ ^3P^o_1$	670.514	671.221	−0.11	1.57[−2]	4.65[5]		
$2p4fF(5/2)_2$	$2p4s\ ^1P^o_1$	758.779	759.057	−0.04	2.71[−3]	6.28[4]		

Table 7
(Continued)

Upper	Lower	λ (nm)			gf	A (s^{-1})		
		Calc.	Obs.	ξ%		Calc.	Exp	σ[a]
$2p4f\,D(5/2)_2$	$2p4s\ ^1P^o_1$	737.777	737.655	0.02	4.56[−2]	1.12[6]		
$2p4f\,D(3/2)_2$	$2p4s\ ^1P^o_1$	733.774	733.589	0.03	3.73[−2]	9.25[5]		
$2p4f\,D(3/2)_1$	$2p4s\ ^3P^o_2$	676.249	676.817	−0.08	5.00[−4]	2.43[4]		
$2p4f\,D(5/2)_2$	$2p4s\ ^3P^o_2$	679.408	680.105	−0.10	3.31[−3]	9.57[4]		
$2p4f\,D(3/2)_2$	$2p4s\ ^3P^o_2$	676.013	676.647	−0.09	4.01[−3]	1.17[5]		
$2p4f\,F(5/2)_3$	$2p4s\ ^3P^o_2$	697.252	698.396	−0.16	2.17[−3]	4.26[4]		
$2p4f\,D(5/2)_3$	$2p4s\ ^3P^o_2$	679.601	680.322	−0.11	3.96[−2]	8.16[5]		
			$2p4f$–$2p4d$					
$2p4f\,D(3/2)_1$	$2p4d\ ^3P^o_0$	12974.039	14081.929	−7.87	9.04[−2]	1.19[4]		
$2p4f\,D(3/2)_1$	$2p4d\ ^3D^o_1$	7677.248	8020.854	−4.28	2.64[−2]	9.97[3]		
$2p4f\,D(3/2)_1$	$2p4d\ ^3P^o_1$	12567.551	13602.666	−7.61	7.81[−2]	1.10[4]		
$2p4f\,F(5/2)_2$	$2p4d\ ^3D^o_1$	11646.596	12608.750	−7.63	2.88[−1]	2.83[4]		
$2p4f\,D(3/2)_2$	$2p4d\ ^3D^o_1$	7646.897	7996.993	−4.38	1.16[−2]	2.65[3]		
$2p4f\,D(5/2)_2$	$2p4d\ ^3P^o_1$	13756.104	15066.367	−8.70	9.77[−2]	6.89[3]		
$2p4f\,D(3/2)_2$	$2p4d\ ^3P^o_1$	12486.265	13534.181	−7.74	9.55[−2]	8.17[3]		
$2p4f\,D(5/2)_2$	$2p4d\ ^1P^o_1$	132082.948	126582.278	4.35	1.16[−2]	8.86[0]		
$2p4f\,D(3/2)_2$	$2p4d\ ^1P^o_1$	66827.052	64876.087	3.01	2.59[−2]	7.73[1]		
$2p4f\,D(3/2)_1$	$2p4d\ ^3F^o_2$	5521.262	5515.933	0.10	1.14[−3]	8.32[2]		
$2p4f\,D(3/2)_1$	$2p4d\ ^3D^o_2$	7845.783	8193.095	−4.24	1.06[−2]	3.82[3]		
$2p4f\,D(3/2)_1$	$2p4d\ ^3P^o_2$	11891.879	12798.853	−7.09	6.94[−3]	1.09[3]		
$2p4f\,F(5/2)_2$	$2p4d\ ^3F^o_2$	7313.898	7356.836	−0.58	5.33[−2]	1.33[4]		
$2p4f\,D(5/2)_2$	$2p4d\ ^3F^o_2$	5739.144	5742.143	−0.05	9.38[−4]	3.80[2]		
$2p4f\,D(3/2)_2$	$2p4d\ ^3F^o_2$	5505.517	5504.638	0.02	5.14[−4]	2.26[2]		
$2p4f\,F(5/2)_2$	$2p4d\ ^1D^o_2$	8843.531	9032.037	−2.09	8.16[−4]	1.39[2]		
$2p4f\,D(5/2)_2$	$2p4d\ ^1D^o_2$	6640.371	6714.113	−1.10	5.03[−2]	1.52[4]		
$2p4f\,D(3/2)_2$	$2p4d\ ^1D^o_2$	6329.635	6391.655	−0.97	4.94[−2]	1.65[4]		
$2p4f\,F(5/2)_2$	$2p4d\ ^3D^o_2$	12038.910	13039.680	−7.67	4.14[−2]	3.81[3]		
$2p4f\,D(5/2)_2$	$2p4d\ ^3D^o_2$	8293.181	8702.311	−4.70	4.50[−2]	8.73[3]		
$2p4f\,D(3/2)_2$	$2p4d\ ^3D^o_2$	7814.087	8168.200	−4.34	1.28[−2]	2.79[3]		
$2p4f\,D(5/2)_2$	$2p4d\ ^3P^o_2$	12950.852	14086.491	−8.06	3.46[−2]	2.75[3]		
$2p4f\,D(3/2)_2$	$2p4d\ ^3P^o_2$	11819.213	12738.204	−7.21	5.30[−2]	5.06[3]		
$2p4f\,F(5/2)_3$	$2p4d\ ^3F^o_2$	7321.984	7372.348	−0.68	5.86[−3]	1.04[3]		
$2p4f\,F(7/2)_3$	$2p4d\ ^3F^o_2$	7194.089	7232.698	−0.53	2.80[−1]	5.15[4]		
$2p4f\,G(7/2)_3$	$2p4d\ ^3F^o_2$	6188.808	6197.400	−0.14	6.17[−1]	1.53[5]		
$2p4f\,F(5/2)_3$	$2p4d\ ^1D^o_2$	8855.278	9055.428	−2.21	3.83[−1]	4.65[4]		
$2p4f\,F(7/2)_3$	$2p4d\ ^1D^o_2$	8668.892	8845.644	−2.00	1.24[−1]	1.57[4]		
$2p4f\,G(7/2)_3$	$2p4d\ ^1D^o_2$	7249.844	7345.002	−1.30	1.45[−1]	2.62[4]		
$2p4f\,D(5/2)_3$	$2p4d\ ^1D^o_2$	6658.854	6735.322	−1.14	4.35[−3]	9.36[2]		
$2p4f\,F(5/2)_3$	$2p4d\ ^3D^o_2$	12060.835	13088.491	−7.85	1.60[−1]	1.05[4]		
$2p4f\,F(7/2)_3$	$2p4d\ ^3D^o_2$	11717.560	12654.704	−7.41	2.07[−1]	1.44[4]		
$2p4f\,G(7/2)_3$	$2p4d\ ^3D^o_2$	9266.123	9792.497	−5.38	6.44[−2]	7.14[3]		
$2p4f\,D(5/2)_3$	$2p4d\ ^3D^o_2$	8322.029	8737.974	−4.76	9.47[−3]	1.30[3]		
$2p4f\,F(5/2)_3$	$2p4d\ ^3P^o_2$	25285.729	30787.229	−17.87	9.78[−4]	1.46[1]		
$2p4f\,D(5/2)_3$	$2p4d\ ^3P^o_2$	13021.342	14180.173	−8.17	3.60[−1]	2.02[4]		
$2p4f\,F(5/2)_2$	$2p4d\ ^3F^o_3$	7706.238	7722.246	−0.21	5.21[−3]	1.17[3]		
$2p4f\,D(5/2)_2$	$2p4d\ ^3F^o_3$	5977.929	5962.354	0.26	1.95[−3]	7.26[2]		
$2p4f\,D(3/2)_2$	$2p4d\ ^3F^o_3$	5724.918	5706.688	0.32	8.42[−4]	3.43[2]		
$2p4f\,F(5/2)_2$	$2p4d\ ^3D^o_3$	12610.818	13675.214	−7.78	8.28[−4]	6.95[1]		
$2p4f\,D(5/2)_2$	$2p4d\ ^3D^o_3$	8560.691	8980.853	−4.68	8.14[−3]	1.48[3]		
$2p4f\,D(3/2)_2$	$2p4d\ ^3D^o_3$	8051.076	8413.118	−4.30	7.22[−3]	1.49[3]		
$2p4f\,F(5/2)_3$	$2p4d\ ^3F^o_3$	7715.216	7739.339	−0.31	3.75[−2]	6.00[3]		
$2p4f\,F(7/2)_3$	$2p4d\ ^3F^o_3$	7573.291	7585.584	−0.16	4.98[−3]	8.27[2]		
$2p4f\,G(7/2)_3$	$2p4d\ ^3F^o_3$	6467.427	6454.694	0.20	1.00[−1]	2.28[4]		
$2p4f\,F(5/2)_3$	$2p4d\ ^3D^o_3$	12634.877	13728.909	−7.97	9.12[−3]	5.45[2]		
$2p4f\,F(7/2)_3$	$2p4d\ ^3D^o_3$	12258.808	13252.405	−7.50	2.58[−2]	1.63[3]		
$2p4f\,G(7/2)_3$	$2p4d\ ^3D^o_3$	9601.260	10146.619	−5.37	8.20[−3]	8.48[2]		
$2p4f\,D(5/2)_3$	$2p4d\ ^3D^o_3$	8591.361	9018.840	−4.74	1.22[−1]	1.58[4]		
$2p4f\,G(7/2)_3$	$2p4d\ ^1F^o_3$	44006.337	54466.231	−19.20	1.28[−3]	6.28[0]		
$2p4f\,D(5/2)_3$	$2p4d\ ^1F^o_3$	28599.211	32590.275	−12.25	1.05[−3]	1.22[1]		
$2p4f\,F(7/2)_4$	$2p4d\ ^3F^o_3$	7546.031	7562.752	−0.22	2.02[−1]	2.63[4]		
$2p4f\,G(7/2)_4$	$2p4d\ ^3F^o_3$	6432.730	6423.103	0.15	6.09[−1]	1.09[5]		
$2p4f\,G(9/2)_4$	$2p4d\ ^3F^o_3$	6031.145	6009.399	0.36	3.84[−1]	7.82[4]		
$2p4f\,F(7/2)_4$	$2p4d\ ^3D^o_3$	12187.542	13182.873	−7.55	4.66[−1]	2.33[4]		
$2p4f\,G(7/2)_4$	$2p4d\ ^3D^o_3$	9524.989	10068.770	−5.40	1.13[−1]	9.22[3]		

Table 7
(Continued)

Upper	Lower	λ (nm)			gf	A (s^{-1})		
		Calc.	Obs.	ξ%		Calc.	Exp	σ[a]
$2p4fG(9/2)_4$	$2p4d\ ^3D^o_3$	8670.245	9088.017	−4.60	6.58[−3]	6.49[2]		
$2p4fG(7/2)_4$	$2p4d\ ^1F^o_3$	42450.227	52295.785	−18.83	5.01[−2]	2.06[2]		
$2p4fG(9/2)_4$	$2p4d\ ^1F^o_3$	29491.565	33512.064	−12.00	1.73[−1]	1.48[3]		
$2p4fF(5/2)_3$	$2p4d\ ^3F^o_4$	8307.373	8290.774	0.20	1.89[−3]	2.61[2]		
$2p4fF(7/2)_3$	$2p4d\ ^3F^o_4$	8143.124	8114.578	0.35	2.00[−3]	2.87[2]		
$2p4fG(7/2)_3$	$2p4d\ ^3F^o_4$	6878.431	6833.775	0.65	2.76[−3]	5.56[2]		
$2p4fD(5/2)_3$	$2p4d\ ^3F^o_4$	6344.171	6302.945	0.65	5.94[−3]	1.41[3]		
$2p4fF(7/2)_4$	$2p4d\ ^3F^o_4$	8111.616	8088.455	0.29	5.69[−2]	6.41[3]		
$2p4fG(7/2)_4$	$2p4d\ ^3F^o_4$	6839.197	6798.374	0.60	1.06[−1]	1.67[4]		
$2p4fG(9/2)_4$	$2p4d\ ^3F^o_4$	6387.083	6336.654	0.80	2.54[−2]	4.62[3]		
$2p4fG(9/2)_5$	$2p4d\ ^3F^o_4$	6432.771	6385.533	0.74	1.54[0]	2.25[5]		

Notes. Obs. are taken from NIST except for those with a superscript. [a,b,c] are referred to Mar et al. (2000), Eriksson (1983), and Marquette et al. (2000). [a]σ are the uncertainties of experimental rates (Mar et al. 2000). The number in the square bracket represents the power of 10.

Table 8
gf Values Scaled with Experimental Transition Energies

Upper	Lower	λ (nm)		gf	
		Calc.	Obs.	Calc.	Scale
$2p4f\ G(7/2)_3$	$2p4d\ ^1F^o_3$	44006.337	54466.231	1.28[−3]	1.03[−3]
$2p4f\ G(7/2)_4$	$2p4d\ ^1F^o_3$	42450.227	52295.785	5.01[−2]	4.07[−2]
$2p4f\ F(5/2)_3$	$2p4d\ ^3P^o_2$	25285.729	30787.229	9.78[−4]	8.04[−4]
$2p4f\ D(5/2)_3$	$2p4d\ ^1F^o_3$	28599.211	32590.275	1.05[−3]	9.20[−4]
$2p4f\ G(9/2)_4$	$2p4d\ ^1F^o_3$	29491.565	33512.064	1.73[−1]	1.53[−1]
$2p4f\ D(5/2)_2$	$2p4d\ ^3P^o_1$	13756.104	15066.367	9.77[−2]	8.92[−2]
$2p4f\ D(5/2)_3$	$2p4d\ ^3P^o_2$	13021.342	14180.173	3.60[−1]	3.31[−1]
$2p4f\ D(5/2)_2$	$2p4d\ ^3P^o_2$	12950.852	14086.491	3.46[−2]	3.18[−2]
$2p4f\ F(5/2)_3$	$2p4d\ ^3D^o_3$	12634.877	13728.909	9.12[−3]	8.40[−3]
$2p4f\ D(3/2)_1$	$2p4d\ ^3P^o_0$	12974.039	14081.929	9.04[−2]	8.33[−2]
$2p4f\ F(5/2)_3$	$2p4d\ ^3D^o_2$	12060.835	13088.491	1.60[−1]	1.47[−1]
$2p4f\ F(5/2)_2$	$2p4d\ ^3D^o_3$	12610.818	13675.214	8.29[−4]	7.64[−4]
$2p4f\ D(3/2)_2$	$2p4d\ ^3P^o_1$	12486.265	13534.181	9.55[−2]	8.81[−2]
$2p4f\ F(5/2)_2$	$2p4d\ ^3D^o_2$	12038.91	13039.68	4.14[−2]	3.82[−2]
$2p4f\ F(5/2)_2$	$2p4d\ ^3D^o_1$	11646.596	12608.75	2.88[−1]	2.66[−1]
$2p4f\ D(3/2)_1$	$2p4d\ ^3P^o_1$	12567.551	13602.666	7.81[−2]	7.22[−2]
$2p4f\ F(7/2)_4$	$2p4d\ ^3D^o_3$	12187.542	13182.873	4.66[−1]	4.31[−1]
$2p4f\ F(7/2)_3$	$2p4d\ ^3D^o_3$	12258.808	13252.405	2.58[−2]	2.38[−2]
$2p4f\ F(7/2)_3$	$2p4d\ ^3D^o_2$	11717.56	12654.704	2.07[−1]	1.92[−1]
$2p4f\ D(3/2)_2$	$2p4d\ ^3P^o_2$	11819.213	12738.204	5.30[−2]	4.92[−2]
$2p4f\ D(3/2)_1$	$2p4d\ ^3P^o_2$	11891.879	12798.853	6.94[−3]	6.45[−3]
$2p4f\ G(7/2)_4$	$2p4d\ ^3D^o_3$	9524.989	10068.77	1.13[−1]	1.07[−1]
$2p4f\ G(7/2)_3$	$2p4d\ ^3D^o_2$	9266.123	9792.497	6.44[−2]	6.09[−2]
$2p4f\ G(7/2)_3$	$2p4d\ ^3D^o_3$	9601.26	10146.619	8.20[−3]	7.76[−3]
$2p4f\ D(5/2)_3$	$2p4d\ ^3D^o_2$	8322.029	8737.974	9.47[−3]	9.02[−3]
$2p4f\ D(5/2)_3$	$2p4d\ ^3D^o_3$	8591.361	9018.84	1.23[−1]	1.17[−1]
$2p4f\ D(5/2)_2$	$2p4d\ ^3D^o_2$	8293.181	8702.311	4.50[−2]	4.29[−2]
$2p4f\ D(5/2)_2$	$2p4d\ ^3D^o_3$	8560.691	8980.853	8.14[−3]	7.76[−3]
$2p4f\ G(9/2)_4$	$2p4d\ ^3D^o_3$	8670.245	9088.017	6.58[−3]	6.28[−3]
$2p4f\ D(3/2)_2$	$2p4d\ ^3D^o_1$	7646.897	7996.993	1.16[−2]	1.11[−2]
$2p4f\ D(5/2)_2$	$2p4d\ ^1P^o_1$	132082.948	126582.278	1.16[−2]	1.21[−2]
$2p4f\ D(3/2)_2$	$2p4d\ ^3D^o_2$	7814.087	8168.2	1.28[−2]	1.22[−2]
$2p4f\ D(3/2)_2$	$2p4d\ ^3D^o_3$	8051.076	8413.118	7.22[−3]	6.91[−3]
$2p4f\ D(3/2)_1$	$2p4d\ ^3D^o_1$	7677.248	8020.854	2.64[−2]	2.53[−2]
$2p4f\ D(3/2)_1$	$2p4d\ ^3D^o_2$	7845.783	8193.095	1.06[−2]	1.01[−2]
$2p4f\ D(3/2)_2$	$2p4d\ ^1P^o_1$	66827.052	64876.087	2.59[−2]	2.67[−2]

Note. The number in the square bracket represents the power of 10.

Table 7. These data are arranged according to different transition arrays like $2p4f$–$2s2p^3$, $2p4f$–$2p3s$, $2p4f$–$2p3d$, and so on. In the present work, we only present results associated with gf values larger than 5×10^{-4} in the Babushkin (length) gauge. The relative difference in wavelengths (ξ%) between the present calculation and NIST values is listed in the fifth column of Table 7. For convenience, this is also illustrated in Figure 2. It can be seen that the difference is about 0.2%

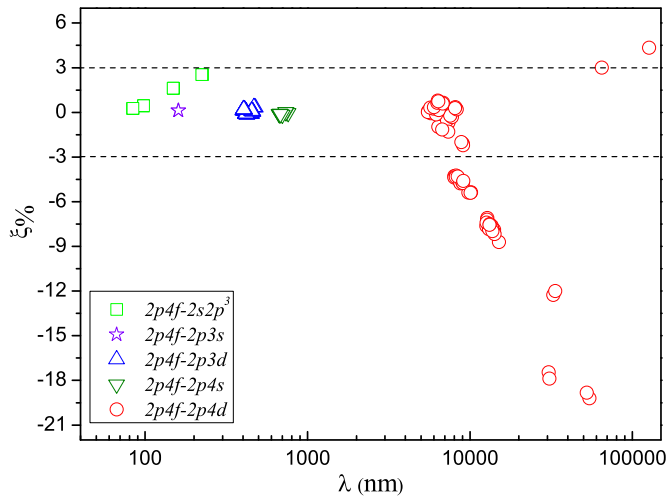

Figure 2. Relative difference (ξ%) in wavelengths between present calculations and NIST values for all transitions from the $2p4f$ configuration.

for the $2p4f$–$2p3s$, $2p4f$–$2p3d$, and $2p4f$–$2p4s$ transitions. Some transitions down to $2s2p^3$, e.g., $^1D^o_2$ and $^1P^o_1$, are off by 1.6%–2.5%. It should be noted that the transitions between states of $2p4f$ and $2p4d$ configurations are exceptions. The transition energies are small and thus very hard to obtain accurately as they result from the subtraction of two equally large numbers.

Transition rates in the Babushkin (length) gauge are presented in the seventh column of Table 7. The available experimental transition rates for the transition $2p4f$–$2p3d$ are also displayed for comparison. It can be shown that present calculations are in reasonable agreement with the measurements by Mar et al. (2000). The only large discrepancy is found for the transition from $4fF(5/2)_2$ to $3d\,^3F^o_2$.

It should be pointed out that the errors in the wavelengths lead to errors in the calculated transition rates, especially for the transitions with large wavelengths, e.g., the $2p4f$–$2p4d$ transitions. The errors in the transitions, however, can be corrected by scaling the rates with experimental wavelengths. We should stress that these lines are hardly observed in experiments due to small branching ratios. Even though they are of little diagnostic importance we still present scaled gf values in Table 8 for lines where the difference in wavelength compared to NIST is larger than 3%. The final scaled results are obviously improved.

Liu pointed out that λ404.1 is the strongest line among the ones from the $2p4f$ configuration (Liu et al. 2000). This is confirmed by our calculations. Moreover, we found that the gf value of the line with $\lambda = 424.1$ nm is large. This may be the reason why there is much work focusing on these two lines (Escalante & Dalgarno 1991; Liu et al. 2000; Fang et al. 2011). In addition, we found that in the infrared region there is a strong line produced by the transition from $4fG(9/2)_5$ to $4d\,^3F^o_4$ with $gf(= 1.54)$.

With regard to plasma diagnostics, accurate atomic data are indispensable. For example, Prueitt used a group of multiplet lines with λ403.51, λ404.13, and λ404.35, namely the transition between $2p4f\,^3G$ and $2p3d^3F^o$, to determine the temperature of plasmas produced by lightnings (Prueitt 1963). The values used to diagnose the plasma in that work deviate substantially from the present results. With respect to the accuracy of present calculations, some analysis based on old atomic data should be re-done.

4. CONCLUSIONS

We calculated the wavelengths and oscillator strengths for the transitions from the $2p4f$ configuration in N^+ using the GRASP2K package based on the MCDHF method. In order to deal with the pair-coupling level structure higher-order electron correlation effects were taken into account through an extended set of reference configurations. Also, the Breit interaction was included to improve fine-structure splittings of the $2p4f$ configuration. Except for some transitions with large wavelengths, uncertainties of the present calculations were controlled within 3% and 5% for wavelengths and oscillator strengths, respectively. We also compared our results with other theoretical and experimental values when available. It was shown that previous calculations within the non-relativistic framework are not well suited for the level structure of the $2p4f$ configuration. Therefore, we recommend our present results based on a fully relativistic method for abundance analysis and plasma diagnosis.

X.Z.S. thanks Professor P. Yuan for the discussion and the financial support by the Research and Development Program for Science and Technology of Hebei Province (grant No.11217168), the Research and Development Program for Science and Technology of Handan (grant Nos. 1128103071, 1121120069-5), the Foundation of Handan College (grant No.09005). J.G.L. and J.G.W. were supported by the National Basic Research program of China under grant No. 2013CB922200 and the National Science Foundation of China under grant No. 11025417.

REFERENCES

Brink, J. A., Coetzer, F. J., Olivier, J. H. I., et al. 1978, ZPhyA, 288, 1
Cowan, R. D. 1981, The Theory of Atomic Structure and Spectra (London: Univ. California Press)
Denis, A., Desesquelles, J., Dufay, M., & Poulizac, M. 1968, Compt. Rend., 266B, 64
Desesquelles, J. 1971, AnPhy, 6, 71
Ekman, J., Godefroid, M. R., & Hartman, H. 2014, Atoms, 2, 215
Eriksson, K. B. S. 1983, PhyS, 28, 593
Escalante, V., & Dalgarno, A. 1991, ApJ, 369, 213
Escalante, V., & Morisset, C. 2005, MNRAS, 361, 813
Fang, X., Storey, P. J., & Liu, X. W. 2011, A&A, 530, A18
Fink, U., McIntire, G. N., & Bashkin, S. 1968, JOSA, 58, 475
Grant, I. P. 2007, Relativistic Quantum Theory of Atoms and Molecules: Theory and Computation (Oxford: Springer)
Grant, I. P., McKenzie, B. J., Norrington, P. H., Mayers, D. F., & Pyper, N. C. 1980, CoPhC, 21, 207
Jönsson, P., Gaigalas, G., Bieroń, J., Froese Fischer, C., & Grant, I. P. 2013, CoPhC, 184, 2197
Jönsson, P., Li, J., Gaigalas, G., & Dong, C. 2010, ADNDT, 96, 271
Kelly, P. S. 1964, JQSRT, 4, 117
Kramida, A., Ralchenko, Yu., Reader, J., & NIST ASD Team., 2013, NIST Atomic Spectra Database (Ver. 5.1), (Gaithersburg, MD: National Institute of Standards and Technology), http://physics.nist.gov/asd (2014 February 24)
Li, J. G., Jönsson, P., Godefroid, M., Dong, C. Z., & Gaigalas, G. 2012, PhRvA, 86, 052523
Liu, X. W., Storey, P. J., Barlow, M. J., et al. 2000, MNRAS, 312, 585
Mar, S., Perez, C., Gonzalez, V. R., et al. 2000, A&AS, 144, 509
Marquette, A., Gisselbrecht, M., Benten, W., & Meyer, M. 2000, PhRvA, 62, 022513
McCrocklin, W. B., Jr., & Head, C. E. 1971, JOSA, 61, 619
Moore, C. E. 1949, in Atomic Energy Levels, Vol. I–II (National. Bureau of Standards Circular 467; Washington, DC: Natl. Bur. Std.)
Olsen, J., Godefroid, M., Jönsson, P., Malmqvist, P. A., & Froese Fischer, C. 1995, PhRvE, 52, 4499
Pinnington, E. H. 1970, NucIM, 90, 93

Prueitt, M. L. 1963, JGR, 68, 803
Shen, X. Z., Yuan, P., & Liu, J. 2010, ChPhB, 19, 053101
Sturesson, L., Jönsson, P., & Froese Fischer, C. 2007, CoPhC, 177, 539
The Opacity Project Team. 1995, The Opacity Project, Vol. 1 (Bristol, UK: Institute of Physics), http://cdsweb.u-strasbg.fr/topbase/topbase.html
Uman, M. A., Orville, R. E., & Salanave, L. E. 1964, JAtS, 21, 306
Victor, G. A., & Escalante, V. 1988, ADNDT, 40, 227
Wallace, L. 1963, ApJ, 139, 994
Wiese, W. L., Smith, M. W., & Glennon, B. M. 1965, NSRDS-NBS-4, Vol. I (Washington, DC: U. S. Govt. Printing)